Journal of Materials Chemistry B

Binding of an amphiphilic phthalocyanine to pre-formed liposomes confers light-triggered cargo release

Journal:	*Journal of Materials Chemistry B*
Manuscript ID	TB-ART-06-2018-001602.R1
Article Type:	Paper
Date Submitted by the Author:	12-Aug-2018
Complete List of Authors:	Machacek, Miloslav; Charels University in Prague, Faculty of Pharmacy in Hradec Kralove, Department of Biochemical Sciences Carter, Kevin; University at Buffalo, Kostelansky, Filip; Charles University in Prague, Faculty of Pharmacy, Department of Pharmaceutical Chemistry and Pharmaceutical Analysis Miranda, Dyego; University at Buffalo Seffouh, Amal; Mcgill University Ortega, Joaquin; Mcgill University Simunek, Tomas; Charels University in Prague, Faculty of Pharmacy in Hradec Kralove, Department of Biochemical Sciences Zimcik, Petr; Charles University in Prague, Faculty of Pharmacy, Department of Pharmaceutical Chemistry and Pharmaceutical Analysis Lovell, Jonathan; University at Buffalo,

Journal Name

ARTICLE

Binding of an amphiphilic phthalocyanine to pre-formed liposomes confers light-triggered cargo release

Received 00th January 20xx,
Accepted 00th January 20xx

DOI: 10.1039/x0xx00000x

www.rsc.org/

Miloslav Macháček[a,b], Kevin A Carter[a], Filip Kostelanský[b], Dyego Miranda[a], Amal Seffouh[c], Joaquin Ortega[c], Tomáš Šimůnek[b], Petr Zimčík[b] and Jonathan F Lovell[a,*]

Liposomes are able to load a range of cargos and have been used for drug delivery applications, including for stimuli-triggered drug release. Here, we describe an approach for imparting near infrared (NIR) light-triggered release to pre-formed liposomes, using a newly-synthesized cationic, amphiphilic phthalocyanine. When simply mixed in aqueous solution with cargo-loaded liposomes, the cationic amphiphilic phthalocyanine, but not a cationic hydrophilic azaphthalocyanine, spontaneously incorporates into the liposome bilayer. This enables subsequent release of loaded cargo (doxorubcin or basic orange) upon irradiation with NIR light. The rate of release could be altered by varying the amount of photosensitizer added to the liposomes. In the absence of NIR light exposure, stable cargo loading of the liposomes was maintained.

Introduction

Drug delivery systems aim to deliver drugs at therapeutically relevant doses while minimizing side effects.[1, 2] To achieve this, nanoparticles such as liposomes have been used to encapsulate anti-cancer agents.[3, 4] The encapsulation can reduce toxicity and enhance therapeutic efficacy.[1, 5] Most existing clinical nanoparticles rely on the enhanced permeability and retention (EPR) effect for drug accumulation in tumors, which enables the passive accumulation of nanoparticles within neoplastic tissue due to the leaky nature of tumor blood vessels.[6-8] However factors including sparse tumor vascularization, tumor interstitial fluid pressure, and poor drug bioavailability limit the efficacy of such approaches.[9-12] To overcome these limitations several strategies have been developed including active targeting and site-specific drug release.[13-17] Site-specific release is of interest as this strategy can increase drug concentration and improve bioavailability in tumors by releasing the drug from the nanoparticle carrier.[15] A large number of site-specific release triggers have been developed, including heat, light, ultrasound, and pH.[18, 19] Light-triggered release is of interest as it offers good spatial and temporal control compared of targeted release.[20-31] Insertion of photosensitizers into liposome bilayers enables the light-triggered release of a large variety of cargos.[32-35] Singlet oxygen generated in the bilayer can oxidize unsaturated lipids, leading to membrane permeabilization.[36, 37]

The structure of liposomes allows for the encapsulation of a wide variety of hydrophilic and hydrophobic small molecules in the aqueous core and bilayer respectively.[38] Hydrophilic compounds can either be entrapped passively or actively using a remote loading gradient.[39, 40] The incorporation of hydrophobic molecules typically occurs during the formation of the liposomes as hydrophobic molecules spontaneously partition into the hydrophobic bilayer. Hydrophobic compounds are not usually incorporated into the liposomal bilayer after the liposomes have already been formed [41] or it takes unusually long time that is not very practical.[42] Such an approach would be of interest as existing nanoparticles, including clinically approved formulations such as Doxil®, and Myocet® could potentially be imparted with active drug release properties without changing the formulation of the liposomes or their preparation process.

Here we report a new strategy to trigger drug release in which the triggering component can simply be mixed with pre-formed liposomes in aqueous solution. To this end, an amphiphilic cationic phthalocyanine is synthesized and is demonstrated to readily insert into pre-formed liposomes upon mixing. The compound is demonstrated to induce light-triggered release with pre-formed liposomes loaded with basic orange 14 (BO14) or doxorubicin (Dox).

Experimental

General

Organic solvents used in synthesis were of analytical grade. Anhydrous butanol for the cyclotetramerization was distilled from magnesium. Unsubstituted zinc phthalocyanine (ZnPc) was

[a] Department of Biomedical Engineering, University at Buffalo, State University of New York, Buffalo, NY, 14260, USA
[b] Faculty of Pharmacy, Charles University, Akademika Heyrovského 1203/8, 500 05 Hradec Králové, Czech Republic
[c] Department of Anatomy and Cell Biology, McGill University Montreal, Quebec, H3A 0C7, Canada

Electronic Supplementary Information (ESI) available: [supporting figures]. See DOI: 10.1039/x0xx00000x

purchased from Sigma-Aldrich. Other chemicals for synthesis were purchased from certified suppliers (i.e., Sigma-Aldrich, TCI Europe, Acros, and Merck) and used as received. TLC was performed on Merck aluminium sheets coated with silica gel 60 F254. Merck Kieselgel 60 (0.040−0.063 mm) was used for column chromatography. Infrared spectra were measured on a Nicolet 6700 spectrometer in ATR mode. ^{1}H and ^{13}C NMR spectra were recorded on VNMR S500 NMR spectrometer. Chemical shifts are reported as δ values in ppm and are indirectly referenced to $Si(CH_3)_4$ *via* the signal from the solvent. *J* values are given in Hz. Elemental analysis was carried out using a Vario Micro Cube Elemental Analyzer (Elementar Analysensysteme GmbH, Hanau, Germany). UV−Vis spectra were recorded using a Shimadzu UV-2600 spectrophotometer or Perkin Elmer Lambda 35. Steady-state fluorescence spectra were measured using FS5 Spectrofluorometer (Edinburg Instruments) or PTI fluorometer. MALDI-TOF mass spectra were recorded in positive reflection mode on a 4800 MALDI TOF/TOF mass spectrometer (AB Sciex, Framingham, MA, USA) in *trans*-2-[3-(4-*tert*-butylphenyl)-2-methyl-2-propenylidene]-malononitrile, which was used as a matrix. The instrument was calibrated externally with a five-point calibration using a Peptide Calibration Mix1 kit (LaserBio Laboratories, Sophia- Antipolis, France). Compounds **1** [43] and **3** [44] were prepared by published methods.

Compound synthesis

*2,3-bis{2,6-bis[(1H-imidazol-1-yl)methyl]-4-methylphenoxy}phthalocyaninato magnesium(II) (**4**):*

Magnesium turnings (1.33 g, 55 mmol) and a small crystal of iodine were refluxed in freshly distilled anhydrous butanol (80 mL) for 3 hours. Phthalonitrile (0.776 g, 6 mmol) and compound **3** (1.32 g, 2 mmol) [44] were then added to the reaction mixture and the reflux continued for 24 h. The reaction mixture was then cooled to room temperature and the solvent was evaporated under the reduced pressure. The crude product was extracted from the residual magnesium butoxide with a mixture of THF/$CHCl_3$ (1:1) and then with pyridine and filtered. The extracts were combined and the solvents were evaporated. The mixture was separated by column chromatography on silica first with mixture of THF/$CHCl_3$/pyridine 1:1:1. The mobile phase was changed to pyridine after elution of symmetrical congener (unsubstituted magnesium phthalocyanine) and the desired product was collected (R_f = 0.55 in pyridine). The purification by column chromatography was repeated once more. The pure product was collected, solvents were evaporated and the solid was washed with ethylacetate, THF and hexane. Green solid, 0.712 g (33%). IR (ATR): ν_{max} = 1507, 1481, 1458, 1404, 1336, 1285, 1083, 1057 cm^{-1}. ^{1}H NMR (500 MHz, $CDCl_3$/pyridine-d_5) δ (ppm) 9.64 – 9.57 (m, 4H, PcH), 9.36 (d, 2H, J = 7,3 Hz, PcH), 8.43 (s, 2H, PcH), 8.29 – 8.14 (m, 6H, PcH), 7.07 (s, 4H, ArH), 6.93 (s, 4H, ArH), 6.86 (s, 4H, ArH), 6.46 (s, 4H, ArH), 5.02 (s, 8H, CH_2), 2.34 (s, 6H, CH_3). ^{13}C NMR (125 MHz, $CDCl_3$/pyridine-d_5) δ (ppm) 155.37; 154.90; 153.85; 151.96; 148.00; 147.11; 139.31; 139.25, 139.07, 137.54; 137.12; 134.01; 130.80; 130.31; 129.69; 129.48; 129.25; 123.22; 122.87; 119.25; 107.20; 45.50; 21.16.

*2,3-bis{2,6-bis[(1H-imidazol-1-yl)methyl]-4-methylphenoxy}phthalocyanine (**5**):*

p-Toluenesulfonic acid monohydrate (0.9 g, 4.74 mmol) in THF (8 mL) was added to a solution of magnesium complex **4** (0.512 g, 0.473 mmol) in THF (2 mL). The mixture was stirred for 2 h at room temperature. THF was evaporated and the water was added to the mixture. Resulting suspension was filtered and the dark solid was collected. Part of the product remained dissolved in the filtrate. For this reason, the solution of sodium hydroxide was added to this green filtrate to basic pH and extracted 3 times with $CHCl_3$. Organic layers were combined, dried with Na_2SO_4, filtered, evaporated and combined with the solid collected from the first filtration. Green solid, 0.441 g (89%). The product was characterized by MS spectra and used directly in the following reaction. MS (MALDI-TOF): m/z 1046.3 $[M]^+$

*2,3-bis{2,6-bis[(1H-imidazol-1-yl)methyl]-4-methylphenoxy}phthalocyaninato zinc(II) (**6**):*

Anhydrous zinc acetate (0.773 g, 4.21 mmol) was added to a solution of metal free **5** (0.441 g, 0.42 mmol) in pyridine (15 mL) and the mixture was refluxed for 2.5 h. The solvent was evaporated and the water was added. Resulting suspension was filtered, and the precipitate was washed thoroughly with water. The crude product was purified by column chromatography on silica with $CHCl_3$/MeOH (5:1). The eluent was changed to pyridine/MeOH (10:1) after elution of residual metal-free **5**. Pure product was dissolved in small volume of $CHCl_3$ with few drops of pyridine and precipitated by dropping into hexane. The fine suspension was collected by filtration, washed with hexane and dried. Green solid, 0.22 g (47%). IR (ATR): ν_{max} = 1610, 1485, 1462, 1406, 1334, 1286, 1230, 1161, 1089, 1058 cm^{-1}. MS (MALDI-TOF): *m/z* 1108.2 $[M]^+$. ^{1}H NMR (**Fig S1**) (500 MHz, pyridine-d_5) δ (ppm) 9.74 – 9.65 (m, 4H, PcH), 9.24 (d, 2H, *J* = 7.4 Hz, PcH), 8.98 (s, 2H, PcH), 8.20 (dd, 2H, *J* = 5.7; 2.8 Hz, PcH), 8.14 (t, 2H, *J* = 7.3 Hz, PcH), 7.94 (t, 2H, *J* = 7.3 Hz, PcH), 7.69 (s, 4H, ArH), 7.31 (s, 4H, ArH), 7.01(s, 4H, ArH), 6.89 (s, 4H, ArH), 5.38 (s, 8H, CH_2), 2.09 (s, 6H, CH_3). ^{13}C NMR (125 MHz, pyridine-d_5) δ (ppm) 155.02, 154.78, 154.20, 152.96, 149.22, 147.66, 139.24, 139.17, 139.01, 137.95, 137.64, 135.08, 134.36, 131.21, 130.08, 129.85, 129.79, 119.88, 107.80, 45.73, 20.8. Elemental analysis (%) calc. for $C_{62}H_{44}N_{16}O_2Zn + 3H_2O$: C 63.94; H 4.33; N 19.24; found C 64.40; H 4.07; N 18.88. UV-vis (DMF, 1 μM) λ_{max} (ε) 344 (42 200), 606 (24 100), 674 nm (153 800 M^{-1}cm^{-1}).

Journal Name

ARTICLE

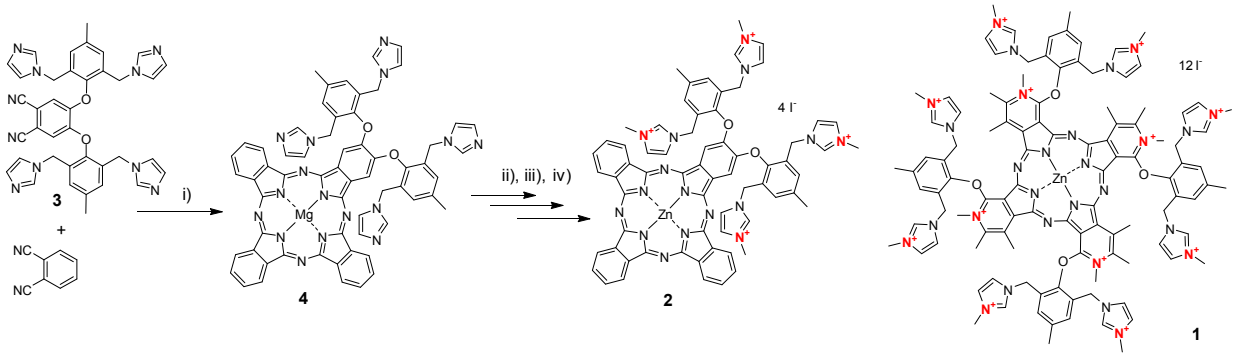

Figure 1: Structures of investigated compounds and their synthesis, including amphiphilic phthalocyanine **2**, and hydrophilic aza-analogue of phthalocyanine **1**. Experimental conditions: i) Mg, I_2, BuOH, reflux, 24 h, 33%; ii) TsOH, THF, room temperature, 2 h, 89%; iii) $Zn(CH_3COO)_2$, pyridine, reflux, 2.5 h, 47%; iv) CH_3I, DMF, 80°C, 24 h, 78%.

*2,3-bis{2,6-bis[(3-methyl-1H-imidazolium-1-yl)methyl]-4-methylphenoxy}phthalocyaninato zinc(II) tetraiodide (**2**):*

Zinc complex **6** (0.2 g, 0.18 mmol) was dissolved in dry DMF (2 mL) under argon atmosphere. Iodomethane (150 µl, 0.342 g, 2.4 mmol) was added and the reaction mixture was stirred for 24 h at 80°C. The solvents were then evaporated. The product was then dissolved in acetone/MeOH 1:1 solution, filtered and precipitated by dropping into diethyl ether (200 mL). The precipitate was collected, washed with diethyl ether and finally with small amount of water. Green solid, 0.237 g (78%). IR (ATR): ν_{max} = 3145, 3084, 1607, 1512, 1484, 1407, 1333, 1286, 1262, 1160, 1092, 1058 cm^{-1}. MS (MALDI-TOF): *m/z* 1548.9 $[M - I^-]^+$. ^1H NMR (**Fig S2**) (500 MHz, DMSO-d_6) δ (ppm) 9.50 – 9.44 (m, 4H, PcH), 9.37 – 9.32 (m, 2H, PcH), 9.26 (s, 4H, PcH), 8.34 – 8.25 (m, 6H, PcH + ArH), 8.11 (s, 2H, ArH), 7.79 (t, 4H, *J* = 1.8 Hz, ArH), 7.65 (s, 4H, ArH), 7.48 (t, 4H, *J* = 1.8 Hz, ArH), 5.71 (s, 8H, CH_2), 3.56 (s, 12H, N^+CH_3), 2.63 (s, 6H, CH_3). ^{13}C NMR (125 MHz, DMSO-d_6) δ (ppm) 154.25, 153.93, 153.12, 151.33, 148.40, 147.42, 138.31, 138.21, 137.96, 137.82, 137.21, 132.87, 132.54, 130.34, 130.14, 128.62, 124.19, 122.96, 122.88, 122.73, 106.72, 47.52, 36.08, 21.11. Elemental analysis (%) calc. for $C_{66}H_{56}I_4N_{16}O_2Zn + H_2O$: C 46.73; H 3.45; N 13.21; found C 46.82; H 3.56; N 12.93. UV-vis (DMF, 1 µM) λ_{max} (ε) 348 (51 000), 607 (31 700), 673 nm (204 000 $M^{-1}cm^{-1}$).

Photophysical characterization

Stock solutions of **1** (1.5 mM) and **2** (10 mM) were prepared in de-ionized water (further referred as "water") or DMSO, respectively. The excitation and emission spectra of **1** and **2** were collected in different environments (demineralized water, Dulbecco's phosphate-buffered saline (dPBS), 0.25% Triton X-100 and liposomes – concentration of lipids in solution 0.65 mg/mL) at concentration of 1µM. Emission spectra were collected using excitation wavelength 370 and 380 nm for **2** and **1**, respectively. For excitation spectra, emission was monitored at 685 and 725 nm for **2** and **1**, respectively.

The singlet oxygen quantum yield (Φ_Δ) and the fluorescence quantum yield (Φ_F) of **2** were determined in DMF *via* the published comparative methods with unsubstituted zinc phthalocyanine (ZnPc, Sigma-Aldrich, Germany) as the reference compound.[45] The following values for ZnPc were used in the calculations: Φ_Δ(DMF) = 0.56 [46] and Φ_F(THF) = 0.32 (λ_{ex} = 600 nm).[47]

Amphiphilic compound **2** was also used for titration experiments dissolved in water or dPBS. Liposomes were gradually added to the 1.5 µM solution of **2** and absorbtion spectra were measured – molar ratios ranging from 1:1 to 500:1 lipids:PS).

The stability of **1** and **2** in solution during laser irradiation (photobleaching) was assessed using power-tunable 665 nm laser diode (RPMC Lasers, O'Fallon, USA) at fluence rate 320 $mW.cm^{-2}$ and fluorescence measurement (λ_{ex} = 370 nm, λ_{em} = 725 nm) with 720 nm high-pass filter (Chroma Technology) to filter out possible undesirable signal from excitation laser. Measurement was conducted for 10 min and laser was switched-on in 1 min of measurement. Lipid concentration was 0.65 mg/mL and lipid to PS molar ratio was 335:1.

Liposome preparation and characterization

Liposomes were prepared using methods previously described.[32] Briefly, the lipids (200 mg) were dissolved in ethanol (2 mL) and heated to 60°C to fully dissolve the lipids. 1,2-dioleoyl-*sn*-glycero-3-phosphocholine (DOPC, Corden LP-R4-070), egg yolk

phosphatidylcholine (EYPC, NOF COATSOME NC-50) and cholesterol (Chol, PhytoChol; Wilshire Technologies) were used. The general lipid molar ratio used was EYPC:Chol 55:45. Liposomes loaded with doxorubicin were formed with DOPC:CHOL 60:40. Subsequently, 250 mM ammonium sulfate (8 mL) pre-warmed to 60 °C was added. The liposomes were then extruded 10 times using a 10 mL nitrogen pressurized extruder (Northern Lipids) using stacked (80, 100 and 200 nm) polycarbonate membranes at 60°C. Excess ammonium sulfate and ethanol were removed by dialysis (MWCO 12,000-14,000, Fisherbrand) buffer exchanged using 10 mM HEPES (pH 7.4) containing 10% sucrose overnight with three buffer changes. Basic Orange 14 (BO14, TCI America) or doxorubicin (Dox; LC Labs) was encapsulated into the liposomes by remote loading by mixing the liposome and cargo stock solution and incubating for 60 minutes at 60°C to produce liposomes with a final cargo concentration of 1.2 mg/mL. For experiments involving PS, stock solutions of **1** or **2** were later added to the liposomes at different molar ratios (ranging from 500:1 to 1:1 lipids:PS) and mixed.

Size and zeta potential of liposomes were tested in dPBS or 10 mM NaCl, respectively, using dynamic light scattering (NanoBrook, ZetaPlus)

Photosensitizer binding

The rate of PS incorporation to lipid membranes was assessed with real-time fluorescence measurement (1 s step). Solutions of **1** and **2** in water or dPBS at concentrations of 3 µM were prepared from stock solutions and fluorescence was measured for 200 s (λ_{ex} = 380 nm, λ_{em} = 725 nm and λ_{ex} = 370 nm, λ_{em} = 685 nm for **1** and **2,** respectively). In 50 s of the measurement, liposomes were added (final concentration 0.65 mg/mL of lipids with molar ratio 335:1 lipids:PS). PS-free experiments were performed as controls.

Binding of the PS to liposomes was further assessed by two methods. Size exclusion chromatography with Sephadex G-75 was used. Liposomes were mixed with **1** or **2** (molar ratio 335:1 lipids:PS) and 500 µL of mixture was added to the column. dPBS was used as mobile phase and 0.5 mL aliquots were collected at room temperature. Each aliquot was diluted 2× by dPBS and absorption spectra were collected. Absorbance at 716 nm and 677 nm was used for time profile of the elution for **1** and **2**, respectively. The same experiment was performed with PS-free liposomes and their respective absorbance were subtracted from experiments with **1** and **2**. Liposomes were monitored as absorbance at 500 nm where both **1** and **2** have negligible absorbance.

Alternatively, centrifugation method was performed on Amicon Ultra-4 Centrifugal Filter Unit (Ultracel-100 regenerated cellulose membrane; Merck, Darmstadt, Germany). Liposomes with **1** or **2** (molar ratio 335:1 lipids:PS, 500 µL) were diluted 2× with dPBS and centrifuged for 5 min at 4000g at 4 °C. The membrane was washed with retentate after centrifugation to prevent mechanical damage to liposomes on cellulose membrane. This step was repeated four-times. Subsequently, dPBS (500 µL) was added to retentate and gently mixed. Centrifugation was performed for 10 min two-times and dPBS (500 µL) was added and mixed gently – this was repeated two times. Samples were diluted 10× and absorption spectra were taken. Compound **1** was monitored at 716 nm, **2** at 677 nm and liposomes at 500 nm.

Light-Triggered drug release

Light-Triggered release of BO14 from liposomes (0.65 mg/mL or 0.065 mg/mL of lipids with different molar ratio of **1** or **2** ranging from 6700:1 to 8.4:1 lipids:PS) in dPBS solution at room temperature was performed with power-tunable 665 nm laser diode (RPMC Lasers, O'Fallon, USA) at fluence rate 320 mW.cm^{-2}. Similar experiments were also performed with Dox (molar ratio ranging from 10:1 to 5:1 lipids:PS) to further confirm different cargo release from liposomes. Cargo release was recorded real-time in a fluorimeter at 25°C with continuous stirring (1 s step). Triton X-100 (0.25% final concentration) was added after laser irradiation to disrupt remaining liposomes to read the total fluorescence. Cargo release was assessed by measuring BO14 and Dox fluorescence (λ_{ex} = 485 nm, λ_{em} = 525 nm, 510/80 nm bandpass filter (Chroma Technology) and λ_{ex} = 480 nm, λ_{em} = 590 nm, 605/55 nm bandpass filter; (Chroma Technology) for BO14 and Dox respectively; before and after laser treatment with Equation 1:

$$\%_{\mathrm{Release}} = \left(\frac{\mathrm{F}_{final}-\mathrm{F}_{initial}}{\mathrm{F}_{X\text{-}100}-\mathrm{F}_{initial}}\right) \times 100 \text{ (Eq. 1)}$$

where F is fluorescence of BO14 or Dox. The superscripts *final*, *initial* and *X-100* correspond to the fluorescence at the end of the experiment, fluorescence at the beginning of the experiment and fluorescence after addition of Triton X-100, respectively.

To visually assess cargo release, a 2.5% agarose gel was prepared in 5 cm petri dishes. After solidification, a round well (diameter: 8 mm; depth: 3 mm) was cut out of the center of the gel. Liposomes loaded with BO14 (Dox does not possess sufficient fluorescence to be visualized this way) were mixed with different molar ratios of **2** (from 3350:1 to 34:1 lipids:PS) and were added to the well and irradiated with a 665 nm laser (fluence rate 320 mW.cm^{-2}) for 5 or 10 min. The plates were stored at room temperature for 48 hours to allow released BO14 to diffuse through the gel. Water (50 µL) was added to the well of each plate every 12 h to facilitate diffusion. After 48 hours, the plates were imaged using an IVIS Lumina II (Perkin Elmer, Waltham, USA) optical *in vivo* imaging system (excitation at 465 nm with GFP emission filter). Release was quantified by measuring the total fluorescence (total radiant efficiency) of each plate using the ROI tools of the IVIS software.

Cryo-electron microscopy

Holey carbon grids (c-flat CF-2/2-2C-T) were prepared by an overnight wash with chloroform. Before the samples were applied, grids were glow discharged at 15 mA for 15 seconds. A volume of 3.6 µL of sample containing either Dox liposomes or Dox liposomes with PS and after laser treatment was deposited in the EM grid. The concentration of both samples was 0.5 mg/mL doxorubicin. Vitrification was performed in a Vitrobot (Thermo Fisher) by

blotting the grids once for 3 seconds and blot force +1 before they were plunged into liquid ethane. Temperature and relative humidity during the vitrification process were maintained at 25°C and 100 %, respectively. Grids were loaded into a Tecnai F20 electron microscope operated at 200 kV using a Gatan 626 single tilt cryo-holder. Images were collected using a defocus range of -2.7 to -3.5 µm in a Gatan Ultrascan 4000 4k x 4k CCD Camera System Model 895 at a nominal magnification 80,000×, which produced images with a calibrated pixel size of 1.41 Å/pixel. Images were collected with a total dose of 25 e - /Å 2. Images were cropped and prepared for figures using Adobe Photoshop software.

Data analysis

Statistical analysis was performed with GraphPad Prism (version 7.04; GraphPad Software, Inc. San Diego, CA).

Results and discussion

Synthesis and characterization of photosensitizers

The studied PS were prepared by either recently published procedures (for water-soluble non-aggregating cationic azaphthalocyanine **1**) [43] or via a novel synthetic approach for unsymmetrical, amphiphilic phthalocyanine **2** (**Fig 1**). This compound was designed to contain flat hydrophobic phthalocyanine core that could easily insert into the lipid bilayer. It also contains four quaternized nitrogens that makes the whole structure amphiphilic and partially soluble in water. Generally, unsymmetrical phthalocyanines are synthesized by co-cyclotetramerization of two different precursors (A and B). Thus, the statistical condensation of phthalonitrile and compound **3** initiated by magnesium butoxide led to the formation of a mixture of six magnesium congeners (AAAA, AAAB, AABB, ABAB, BBBA, and BBBB), of which the AAAB-type molecule **4** was of interest and was isolated by column chromatography in good yield of 33%. The magnesium complex was then converted to metal-free **5** by *p*-toluenesulfonic acid in THF in good yield of 89%. The metal-free form was converted to zinc complex **6** by zinc acetate in pyridine in yield of 47% and finally alkylated by iodomethane in dry DMF under argon atmosphere (78% yield).

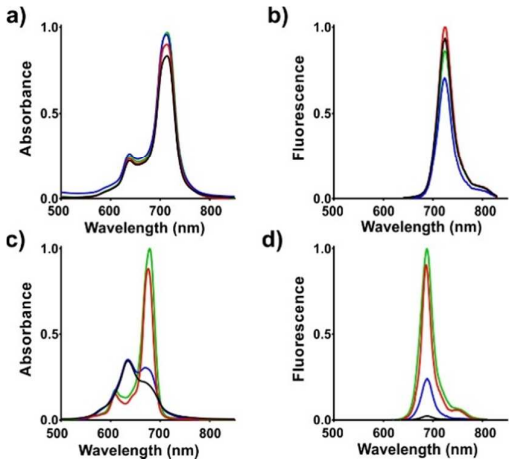

Figure 2. Spectral properties of **1** and **2** in different media. Blue lines: deionized water; Black lines: dPBS; Red lines: liposomes; Green lines: water with Triton X-100. Absorption of 1 µM compound **1** (A) or **2** (C). Fluorescence emission of **1** (B) (λ_{ex} = 380 nm) or **2** (D) **2** (λ_{ex} = 370 nm).

Compound **1** is a polycationic tetra(3,4-pyrido)porphyrazine and is highly water soluble with practically no distribution to lipophilic phases.[43] Phthalocyanine **2** is sparingly water soluble, producing a weakly green saturated water solution but it dissolves well in DMSO and DMF. The amphiphilic nature of **2** suggests that in water-based media it would likely form dimers or aggregates with low fluorescence and singlet oxygen generating properties.[43] To test this hypothesis UV–vis spectroscopy was used to assess the absorption spectra of **1** and **2** dissolved in different media: de-ionized water, dPBS, a surfactant (0.25% Triton X-100), and a liposomal solution. For **1,** there were no significant differences in the absorption (**Fig 2A** and **S3**) and fluorescence excitation and emission (**Fig 2B** and **S3**) spectra. On the other hand, amphiphilic **2** showed changes in all spectra (**Fig 2 C,D** and **S4**). Particularly, a drastic increase in the absorbance in 670-680 nm region (differences in maxima position due to solvatochromic effect), a decrease at 635 nm (**Fig 2C**) and an increase in the emission spectra at 688 nm (**Fig 2D**) in the surfactant and liposome solutions suggest a more monomeric form. **2** appeared slightly more monomeric in water compared to dPBS, based on the higher absorbance at 672 nm and a higher fluorescence signal (**Fig 2C**). The spectral properties were consistent with **2** inserting itself into the hydrophobic bilayer of liposomes, which would be helpful in terms for imparting light-triggered release.

Table 1. Photophysical properties of the photosensitizers in DMF.

Compound	λ_{max}	logε	λ_F	Φ_F	Φ_Δ
1[a]	710	5.28	721	0.13	0.69
2	673	5.31	681	0.25	0.57

[a]Data for compound **1** from ref [43]

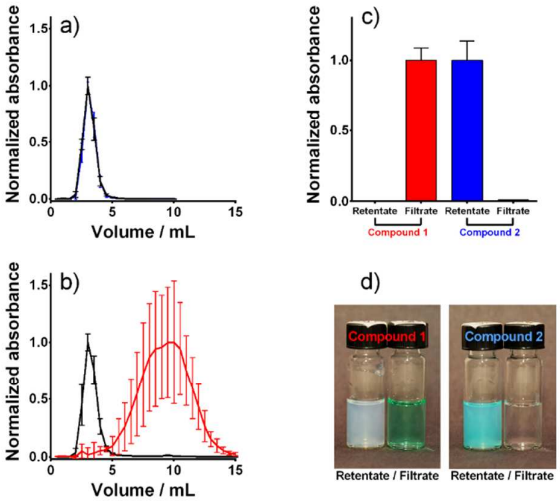

Figure 3. PS binding to liposomes evaluated by size exclusion chromatography for (A) compound **2** and (B) compound **1** and (C) by centrifugal filtration. (D) photographs of filtrate and retentate of samples separated with centrifugal filtration. Lipids:PS molar ratio was 335:1. Black line: liposomes, red line: compound **1**, blue line: compound **2**.

Both studied compounds were also characterized from the photophysical point of view in DMF where both compounds are found exclusively in monomeric form (Table 1). Both PS are able to produce efficiently singlet oxygen and fluorescence. The production of singlet oxygen is of particular importance in the intended application since it is the species that is destroying liposomal membrane and leads to release of the liposomal content.

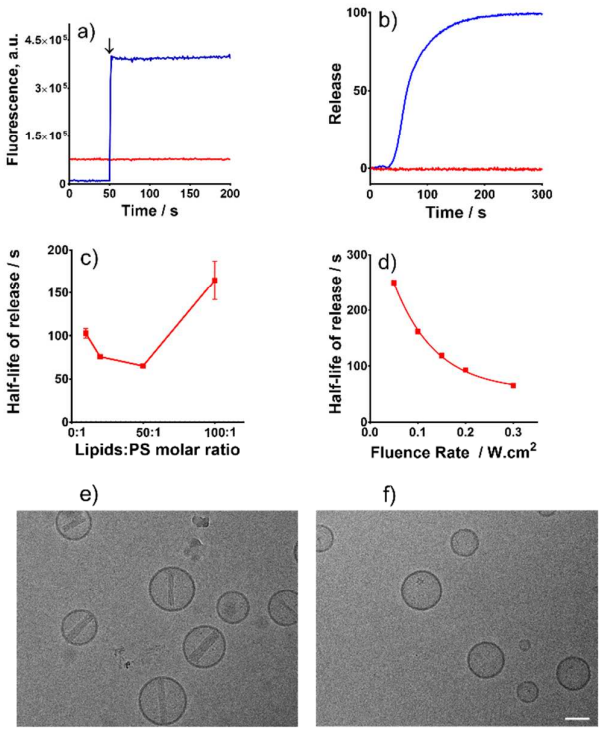

Figure 4. Light-triggered cargo release following photosensitizer binding. (A) Real-time fluorescence measurements of **1** (red line) and **2** (blue line) incorporation into liposomes. Arrow shows addition of liposomes to the solution. (B) Light-triggered release of Dox from liposomes mixed with **1** (red line) and **2** (blue line). Lipids:PS molar ratio is 50:1. (C) Half-life of release of Dox triggered by **2** as a function of the molar ratio of lipids:PS. (D) Half-life of Dox release plotted against fluence rate. Cryo-TEM images of Dox-loaded liposomes (E) before treatment and (F) after PS insertion and laser treatment. Scale bar, 50 nm.

Photosensitizer binding to liposomes

The results of the solubility studies suggested that when solubilized in a liposomal dispersion the amphiphilic **2** is integrated into the liposomal bilayer which is indicated by changes in absorption and fluorescence spectra, similar to the changes observed in the Triton X-100 solution (**Fig 2** and **S4**). To verify this hypothesis, **1** and **2** were mixed with a colloidal liposome solution and incorporation of each compound into the liposomes was tested using size exclusion chromatography and microcentrifugal filtration. Results of the size exclusion chromatography experiments demonstrated that **2** was integrated into the liposomes because the liposomal fraction was eluted together with signal for this compound (**Fig 3A**). On the other hand, polycationic **1** was not incorporated as indicated by the majority of the compound eluting later than the liposomes (**Fig 3B**). Centrifugal filtration studies confirmed these results with **2** being retained in the rententate together with liposomes, while **1** was collected in the filtrate as verified by absorbance (**Fig 3C**) and visually (**Fig 3D**).

To assess whether PS binding impacts liposomal physical parameters, size and polydispersity measurements were performed of the liposomes with or without **2** (**Table 2**). Overall, the size of the liposomes remained close 100 nm in diameter with low polydispersity. Thus, PS insertion did not induce liposomes aggregation. Liposome size and polydispersity remained stable over a one month storage period, with or without **2** inserted. Liposome size and polydispersity were also stable and monodisperse with a wide range of lipid:**2** ratios (**Table S1**). Unexpectedly, a slight trend towards more negative surface charge was observed with increased ratios of **2**. Further experiments would be required to better understand that phenomenon, which might possibly relate to buffer counter ions or other measurement conditions.

Table 2: Size stability of liposomes in refrigerated storage with or without compound **2** (50:1 lipids:PS molar ratio)**.**

	Diameter (nm)	Polydispersity index
Day 1 liposomes	88 ± 1.5	0.078 ± 0.03
Day 1 liposomes + **2**	102 ± 2.6	0.15 ± 0.01
Day 7 liposomes	106 ± 7.6	0.09 ± 0.03
Day 7 liposomes + **2**	104 ± 2.0	0.09 ± 0.05
Day 14 liposomes	89 ± 0.6	0.09 ± 0.03
Day 14 liposomes + **2**	95 ± 0.8	0.12 ± 0.006
Day 21 liposomes	98 ± 1.5	0.13 ± 0.02
Day 21 liposomes + **2**	109 ± 2.0	0.13 ± 0.08

The rate of liposome incorporation was studied for both **1** and **2** with real-time measurements. Compounds were diluted in dPBS and fluorescence measured continuously for 50 seconds at which point liposomes were added. An immediate fluorescence increase was observed for **2** while no significant increase was seen with **1** (**Fig 4A**). Taken together, we can conclude that hydrophilic **1** does not bind the liposomes, whereas amphiphilic **2** rapidly inserts into the lipidi bilayer in a largely monomeric form.

Titration of 1.5 µM solution of **2** in dPBS was performed with gradual addition of liposomes revealed monomerization of **2** in liposomal membrane observed by changes in absorption spectra. Particularly, increase in absorbance at 676 nm and decrease 635 nm with isosbestic points at 608, 658 and 697 nm suggest liposome

concentration-dependent monomerization of **2** (**Fig 5A**). Analogous results were obtained when the liposomes were added in deionized water (**Fig S5**). Similar results were obtained when **2** was gradually added to the solution of 0.065 mg/mL liposomes (**Fig S6**). Similarly, an increase in fluorescence around 686 nm can be observed (**Fig 5B**). Interestingly **2** was rapidly photobleached following laser irradiation which can be observed both as a decrease in fluorescence (**Fig 5C** and **S7**), changes in absorbance (**Fig S8**) and visually (**Fig 5D**). Compound **1** was more stable from the photobleaching point of view (**Fig S7**).

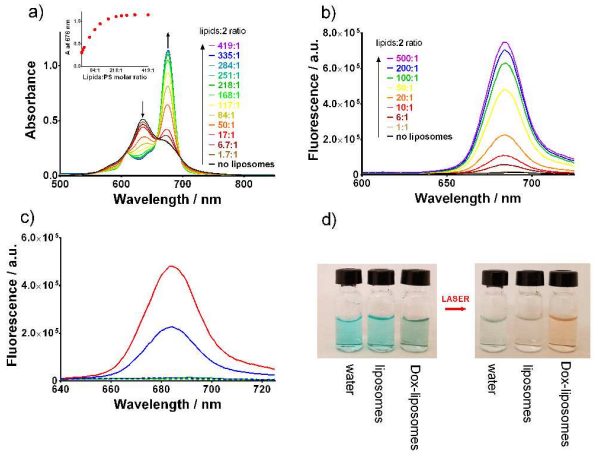

Figure 5. (A) Absorbance and (B) Fluorescence emission with liposome titration to a solution of **2** in dPBS. Molar ratios of lipids to **2** are specified. Inset: change of absorbance at 676 nm. (C) Fluorescence of **2** before (solid lines) and after (dashed lines) laser irradiation. Red: in liposomes, 50:1 lipids:PS molar ratio; blue: in liposomes, 20:1 lipids:PS molar ratio; green: PS only. (D) Photographs of **2** dissolved in water or mixed with empty or dox-loaded liposomes before (left) and after laser treatment (right).

Light-triggered cargo release

The capacity for the PS to impart light-triggered release was assessed with pre-formed liposomes loaded with BO14 or Dox. The pre-formed liposomes were mixed with **1** and **2** at a different lipids:PS molar ratios and were then irradiated with a 665 nm laser at a fluence rate of 320 mW/cm^2. Cargo release was monitored in real-time. Only the liposomes mixed with **2** were able to release the BO14 (**Fig S9**) or Dox (**Fig 4B** and **S10**) while the liposomes mixed with **1** showed no significant release (**Fig 4B** and **S11**). The results indicate that only the PS incorporated in the liposomal membrane are able to induce the damage to the liposomes with their subsequent opening. The results are not unexpected considering the spatial distribution of the highly hydrophilic compound in aqueous environment and a very short half-life of singlet oxygen in this solvent.[48] Thus, despite compound **1** being a good singlet oxygen producer in water [43], this reactive species will be produced far from the target lipid membrane. On the other hand, amphiphilic **2** produces singlet oxygen directly in the membrane, and the produced singlet oxygen likely has a longer half-life in the hydrophobic bilayer.

To further study the effects of **2** on light triggered release, cargo-loaded liposomes were mixed with **2** at different lipids:PS ratios and the release half-life was measured. An optimal lipids:PS ratio was found to be 50:1 for Dox (**Fig 4C** and **S9A**). The release was then studied at various fluence rates using this ratio. The results show that the rate of release could be modified by varying the fluence rate but the fluence requirement for 50% release was the same for all fluence rates (**Fig 4D** and **S10B**). The effects of laser treatment with **2** on liposome morphology was studied using cryogenic transmission electron microscopy (Cryo-TEM). Prior to laser treatment the liposomes were observed to be round with crystalline-like Dox aggregates in the aqueous core (**Fig 4E**). After mixing with **2** and laser treatment, the liposome shape was maintained; however the Dox crystals were no longer present, indicating release of the Dox (**Fig 4F**).

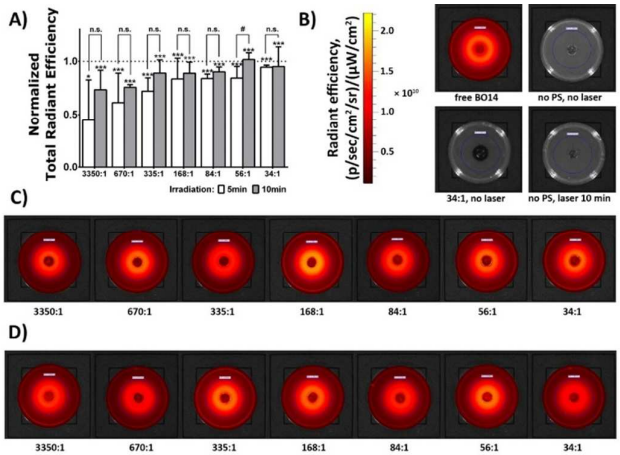

Figure 6. Release of BO14 from liposomes in 2.5% agarose gel. A) Release expressed as mean with SD. The experiments were performed in quadruplicate. One-way ANOVA with Bonferroni's multiple comparison *post hoc* test was used. The results were compared with the control samples (100 %), and the mean values were considered significant if (*) $p < 0.05$, (**) $p < 0.01$, and (***) $p < 0.001$. Statistical significance between groups was assessed using unpaired t-test with Welch's correction and difference between groups was considered significant if (#) $p < 0.05$, (##) $p < 0.01$, and (###) $p < 0.001$. Representative images of the samples: B) Control experiments. Free BO14 was used as positive control (100 %) C) irradiation time 5 min D) irradiation time 10 min.

To visualize the cargo release with this approach, an agarose gel system was used with liposomal BO14, which is strongly fluorescent when released. Solution of liposomes containing **2** in different molar ratios were added to the well cut in 2.5% agarose gel and irradiated for 5 or 10 min with 665 nm laser at a fluence rate of 320 mW/cm^2. After the release from liposomes, the free BO14 was enabled to diffuse to surrounding agarose gel forming a circular area around the well. Lipids:PS molar ratio-dependent increase was observed with higher efficiency in higher molar ratio (lower amount of **2**) observed with 10 min irradiation (**Fig 6**). On the other hand, differences between 5 and 10 min irradiation times was not statistically significant due to higher variability in release.

Control experiments using free BO14 without encapsulation into the liposomes (**Fig 6B**, free BO14) were performed and represented 100% release. Negative controls; compound **2**-free liposomes with and without irradiation (**Fig 6B, Fig S12** no PS, no laser) and compound **2**-containing liposomes without irradiation (**Fig 6B**, **Fig S12** 34:1, no laser) – were also performed showing no release of BO14. This further confirms that BO14 release from liposomes is light-triggered and compound **2**-dependent (**Fig 6A**) and that the **2** alone is not affecting liposomal stability and is not triggering the release of encapsulated drug in the dark (**Fig S10**).

Conclusion

This work establishes that conventional, pre-formed liposomes can be converted into photoactivatable ones by imparting light-triggered cargo release with the binding of a amphiphilic PS. This approach has the advantage enabling the introduction of light-triggered properties to existing liposome formulations such as doxorubicin-loaded liposomes without the need to alter the existing liposomes or produce them in house. We demonstrated proof of principle in which cargo-loaded liposomes are conferred with light-triggered release properties though the mixing of the liposome solution with a PS without disrupting the stability of the liposomes. While this approach may be useful for early stage research or possibly even early stage clinical studies, eventually a stably integrated formulation would be desirable to avoid an additional step of on-site mixing of liposomes and PS. Further studies are needed to advance this approach, including assessment of serum stability of the PS insertion, toxicity, and *in vivo* efficacy.

Conflicts of interest

The authors declare no conflicts.

Acknowledgements

This work was supported by the National Institutes of Health (R01EB017270; DP5OD017898) and the National Science Foundation (1555220). This work was also supported by project EFSA-CDN (No. CZ.02.1.01/0.0/0.0/16_019/0000841) co-funded by ERDF (European Regional Development Fund).

References

1. T. M. Allen and P. R. Cullis, *Science*, 2004, **303**, 1818-1822.
2. J. D. Kingsley, H. Dou, J. Morehead, B. Rabinow, H. E. Gendelman and C. J. Destache, *J. Neuroimmune Pharmacol.*, 2006, **1**, 340-350.
3. Y. Barenholz, *J. Control. Release*, 2012, **160**, 117-134.
4. T. M. Allen and P. R. Cullis, *Adv Drug Deliv Rev*, 2013, **65**, 36-48.
5. A. Z. Wang, R. Langer and O. C. Farokhzad, *Annu. Rev. Med.*, 2012, **63**, 185-198.
6. J. Fang, H. Nakamura and H. Maeda, *Adv Drug Deliv Rev*, 2011, **63**, 136-151.
7. H. Maeda, *J. Control. Release*, 2012, **164**, 138-144.
8. V. Torchilin, *Adv Drug Deliv Rev*, 2011, **63**, 131-135.
9. U. Prabhakar, H. Maeda, R. K. Jain, E. M. Sevick-Muraca, W. Zamboni, O. C. Farokhzad, S. T. Barry, A. Gabizon, P. Grodzinski and D. C. Blakey, in *Cancer Res.*, (c)2013 AACR., United States, 2013, vol. 73, pp. 2412-2417.
10. D. Needham and M. W. Dewhirst, *Adv Drug Deliv Rev*, 2001, **53**, 285-305.
11. A. I. Minchinton and I. F. Tannock, *Nat. Rev. Cancer*, 2006, **6**, 583-592.
12. D. Luo, K. A. Carter and J. F. Lovell, *Wiley Interdiscip Rev Nanomed Nanobiotechnol*, 2015, **7**, 169-188.
13. R. K. Jain and T. Stylianopoulos, *Nat. Rev. Clin. Oncol.*, 2010, **7**, 653-664.
14. A. A. Manzoor, L. H. Lindner, C. D. Landon, J.-Y. Park, A. J. Simnick, M. R. Dreher, S. Das, G. Hanna, W. Park, A. Chilkoti, G. A. Koning, T. L. M. t. Hagen, D. Needham and M. W. Dewhirst, 2012, DOI: 10.1158/0008-5472.CAN-12-1683.
15. S. Ganta, H. Devalapally, A. Shahiwala and M. Amiji, *J. Control. Release*, 2008, **126**, 187-204.
16. O. M. Koo, I. Rubinstein and H. Onyuksel, *Nanomedicine*, 2005, **1**, 193-212.
17. A. I. Freeman and E. Mayhew, *Cancer*, 1986, **58**, 573-583.
18. B. P. Timko, T. Dvir and D. S. Kohane, *Adv. Mater.*, 2010, **22**, 4925-4943.
19. S. Mura, J. Nicolas and P. Couvreur, *Nat Mater*, 2013, **12**, 991-1003.
20. N. Fomina, J. Sankaranarayanan and A. Almutairi, *Adv Drug Deliv Rev*, 2012, **64**, 1005-1020.
21. D. Miranda and J. F. Lovell, *Bioengineering & Translational Medicine*, 2016, **1**, 267-276.
22. D. Luo, K. A. Carter, D. Miranda and J. F. Lovell, *Advanced Science*, 2017, **4**, 1600106.
23. J. Xu, X. Zhou, Z. Gao, Y.-Y. Song and P. Schmuki, *Angew. Chem. Int. Ed.*, 2016, **55**, 593-597.
24. X. Sun, C. Wang, M. Gao, A. Hu and Z. Liu, *Adv. Funct. Mater.*, 2015, **25**, 2386-2394.
25. C. J. Carling, M. L. Viger, V. A. Huu, A. V. Garcia and A. Almutairi, *Chem. Sci.*, 2015, **6**, 335-341.
26. J. Shao, M. Xuan, T. Si, L. Dai and Q. He, *Nanoscale*, 2015, **7**, 19092-19098.
27. T. Lajunen, L.-S. Kontturi, L. Viitala, M. Manna, O. Cramariuc, T. Róg, A. Bunker, T. Laaksonen, T. Viitala, L. Murtomäki and A. Urtti, *Mol. Pharm.*, 2016, **13**, 2095-2107.
28. M. Zan, J. Li, M. Huang, S. Lin, D. Luo, S. Luo and Z. Ge, *Biomaterials Science*, 2015, **3**, 1147-1156.
29. A. M. Goodman, O. Neumann, K. Nørregaard, L. Henderson, M.-R. Choi, S. E. Clare and N. J. Halas, *Proceedings of the National Academy of Sciences*, 2017, DOI: 10.1073/pnas.1713137114.
30. Y. Dai, H. Bi, X. Deng, C. Li, F. He, P. a. Ma, P. Yang and J. Lin, *Journal of Materials Chemistry B*, 2017, **5**, 2086-2095.
31. J. Song, X. Yang, O. Jacobson, L. Lin, P. Huang, G. Niu, Q. Ma and X. Chen, *ACS Nano*, 2015, **9**, 9199-9209.
32. D. Luo, K. A. Carter, A. Razi, J. Geng, S. Shao, D. Giraldo, U. Sunar, J. Ortega and J. F. Lovell, *Biomaterials*, 2016, **75**, 193-202.
33. K. A. Carter, S. Shao, M. I. Hoopes, D. Luo, B. Ahsan, V. M. Grigoryants, W. Song, H. Huang, G. Zhang, R. K. Pandey, J.

Geng, B. A. Pfeifer, C. P. Scholes, J. Ortega, M. Karttunen and J. F. Lovell, *Nat Commun*, 2014, **5**, 3546.

34. B. Q. Spring, R. B. Sears, L. Z. Zheng, Z. Mai, R. Watanabe, M. E. Sherwood, D. A. Schoenfeld, B. W. Pogue, S. P. Pereira, E. Villa and T. Hasan, *Nature nanotechnology*, 2016, **11**, 378-387.
35. D. Miranda, K. Carter, D. Luo, S. Shao, J. Geng, C. Li, U. Chitgupi, S. G. Turowski, N. Li, G. E. Atilla-Gokcumen, J. A. Spernyak and J. F. Lovell, *Adv Healthc Mater*, 2017, **6**.
36. D. Luo, N. Li, K. A. Carter, C. Lin, J. Geng, S. Shao, W. C. Huang, Y. Qin, G. E. Atilla-Gokcumen and J. F. Lovell, *Small*, 2016, **12**, 3039-3047.
37. D. Miranda, N. Li, C. Li, F. Stefanovic, G. E. Atilla-Gokcumen and J. F. Lovell, *ACS Applied Nano Materials*, 2018, DOI: 10.1021/acsanm.8b00435.
38. G. Bozzuto and A. Molinari, in *Int J Nanomedicine*, 2015, vol. 10, pp. 975-999.
39. A. Akbarzadeh, R. Rezaei-Sadabady, S. Davaran, S. W. Joo, N. Zarghami, Y. Hanifehpour, M. Samiei, M. Kouhi and K. Nejati-Koshki, in *Nanoscale Res Lett*, 2013, vol. 8, p. 102.
40. A. Cern, A. Golbraikh, A. Sedykh, A. Tropsha, Y. Barenholz and A. Goldblum, *J. Control. Release*, 2012, **160**, 147-157.
41. A. Sharma and U. S. Sharma, *Int. J. Pharm.*, 1997, **154**, 123-140.
42. P. Zimcik, M. Miletin, K. Kopecky, Z. Musil, P. Berka, V. Horakova, H. Kucerova, J. Zbytovska and D. Brault, *Photochem. Photobiol.*, 2007, **83**, 1497-1504.
43. M. Machacek, J. Demuth, P. Cermak, M. Vavreckova, L. Hruba, A. Jedlickova, P. Kubat, T. Simunek, V. Novakova and P. Zimcik, *J. Med. Chem.*, 2016, **59**, 9443-9456.
44. S. Makhseed, M. Machacek, W. Alfadly, A. Tuhl, M. Vinodh, T. Simunek, V. Novakova, P. Kubat, E. Rudolf and P. Zimcik, *Chem. Commun.*, 2013, **49**, 11149-11151.
45. V. Novakova, M. Miletin, T. Filandrová, J. Lenčo, A. Růžička and P. Zimcik, 2014, DOI: 10.1021/jo402791c.
46. U. Michelsen, H. Kliesch, G. Schnurpfeil, A. K. Sobbi and D. Wohrle, *Photochem. Photobiol.*, 1996, **64**, 694-701.
47. P. Zimcik, V. Novakova, K. Kopecky, M. Miletin, R. Z. Uslu Kobak, E. Svandrlikova, L. Vachova and K. Lang, *Inorg. Chem.*, 2012, **51**, 4215-4223.
48. P. R. Ogilby, *Photochem. Photobiol. Sci.*, 2010, **9**, 1543-1560.

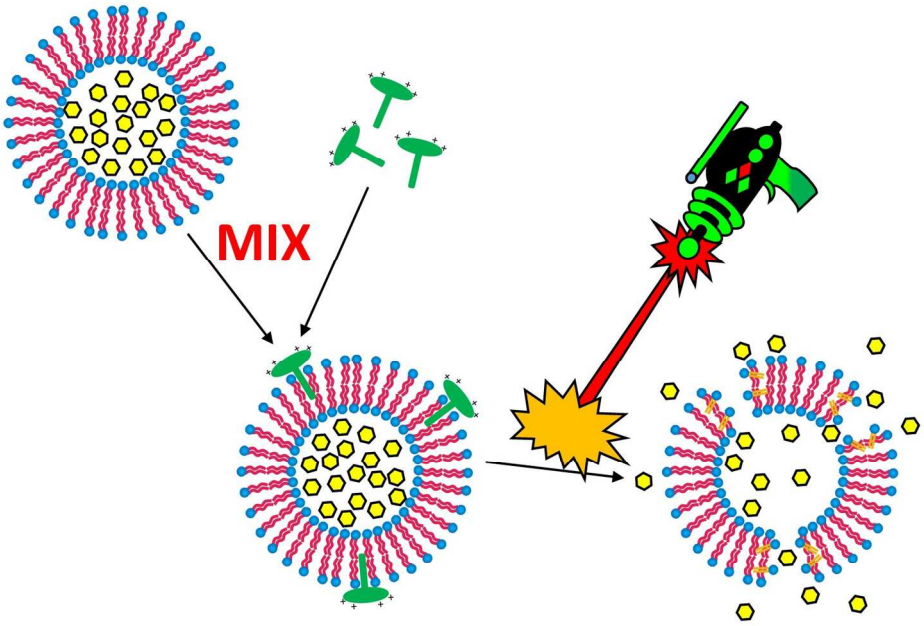

297x209mm (150 x 150 DPI)